A Simple Model of Current Ramp-Up and Ramp-Down in Tokamaks

Richard Fitzpatrick [a]

Institute for Fusion Studies, Department of Physics,

University of Texas at Austin, Austin TX 78712

A simple model of the ramp-up and ramp-down of the toroidal current in a tokamak plasma is developed. Faraday's law of electric induction is found to limit how rapidly the current can be safety ramped up or down. It is estimated that the minimum completely safe ramp-up/down times for the JET, SPARC, and ITER tokamaks are 4.2, 2.0, and 14.7 seconds, respectively. The JET ramp time is in accordance with operational experience. The SPARC and ITER minimum safe ramp times are less than the ramp times in the respective designs. Hence, there is no indication that the design ramp times are infeasible, as was recently suggested in arXiv:2507.05456 (2025). The typical ratios of the inductive electric field to the Connor-Hastie field in SPARC and ITER are found to be less than those in JET. Thus, the fact that the JET tokamak was able to operate successfully without encountering runaway electron problems during current ramps suggests that the future SPARC and ITER tokamaks should also be able to avoid such problems.

---

[a] rfitzp@utexas.edu

I. INTRODUCTION

In a recent paper, Boozer[1] argues that Faraday's law of electric induction places strong constraints on the operation of a future tokamak fusion power plant. In particular, Boozer takes issue with the claim by de Vries et alia (2018)[2] that a fully controlled current ramp-down in the future ITER tokamak, starting from a toroidal plasma current of 15 MA, can be effected in 60 seconds. (Indeed, in an earlier study Boozer[3] seems to argue that the true ramp time is 1000 seconds.) Boozer also takes issue with the claim by Creely et alia[4] that the plasma current in the future SPARC tokamak can be ramped up in 7 seconds, and ramped down in 12 seconds, and seems to imply that the true ramp time is, in fact, 1157 seconds. The claim by de Vries et alia (2018) is made in Sect. 2 of Ref. 2, and is based on simulations performed using the CORSICA[5,6] code. The claim by Creely et alia is deduced from in Fig. 3 of Ref. 4, and is based on simulations made with the TSC[7] code. While it is the case that the CORSICA and TSC codes both have a proven track records, we can certainly agree with Boozer that neither de Vries et alia (2018) or Creely et alia provide sufficient information to validate their claims. To help clarify the situation, this paper presents a simple model of current ramp-up and ramp-down in tokamak plasmas. The aim of the paper is to determine, in a transparent manner, whether the claims by de Vries et alia (2018) and Creely et alia are, at least, plausible, and also to clarify the constraints that Faraday's law actually do place on future tokamak operation. Boozer[1,3] also highlights the danger of runaway electron generation during current ramps, so we shall additionally try to estimate the likelihood of dangerous levels of runaway electron generation during current ramps in future tokamaks.

II. TOKAMAK OPERATION

Figure 1 is a cartoon that illustrates how a toroidal current ramp-up is effected in a conventional tokamak plasma.[8–11] After the initial burn-through phase, the fully ionized plasma starts off as an *ohmic* discharge of circular poloidal cross-section, and relatively small minor radius, that is limited on the first wall, and carries a comparatively small toroidal current. As the toroidal current is gradually increased, the minor radius and vertical

elongation of the plasma increase in concert, but the plasma remains limited on the first wall. (See Fig. 7 of Ref. 8 and Fig. 1 of Ref. 9.) Only in the very final stages of the current ramp is the magnetic X-point added to the equilibrium, at which point the plasma becomes magnetically diverted, and consequently ceases to be limited by the first wall.

The current ramp usually takes place in two stages. (See Fig. 3 of Ref. 4.) In the first stage, the edge safety-factor, q_a, of the plasma is allowed to decrease from an initially very large value to its final value of about 3.5, at fixed plasma minor radius. In the second stage, which is usually much longer in duration than the first, q_a is held constant while the plasma expands in volume. The first stage is hazardous because, as q_a passes through integer values (6, 5, 4, et cetera), the plasma becomes momentarily susceptible to both tearing and ideal-kink modes.[12–14] However, the degree of the hazard is mitigated by the smallness of the plasma current. In the second stage, the safety-factor profile is held approximately constant, and is designed to be stable to both tearing and ideal-kink modes.

After the current ramp has been completed, and the magnetic diverter is operational, external heating is applied to the plasma discharge, while the current is held constant. Consequently, the plasma eventually attains its peak temperature. The current flat-top phase of the plasma discharge is usually much longer in duration than both the current ramp-up and ramp-down phases. Toward the end of the current flat-top, the external heating is turned off, and the plasma eventually returns to the same state that it was in at the end of the current ramp-up. At this point, the sequence of events that constitute the current ramp-up is carried out in reverse order to effect a current ramp-down. In other words, the magnetic X-point is first removed from the plasma, which then becomes limited by the first wall. The plasma is then gradually crushed against the first wall, while the current is reduced, but q_a is held constant. (See Fig. 7 of Ref. 8.) Finally, q_a is allowed to rise to a large value, at fixed minor radius, as last remnants of the plasma current disappear.

III. ANALYSIS

A. Coordinates

Let us model a tokamak plasma, in the simplest imaginable manner, as a periodic cylinder. Let r, θ, z be conventional cylindrical coordinates, and let the magnetic axis of the plasma correspond to $r = 0$. The system is assumed to be periodic in z with period length $2\pi R_0$, where R_0 is the simulated major radius of the plasma. Let a be the minor radius of the plasma at the end of the current ramp.

B. Fundamental Equations

The equilibrium magnetic field is represented as

$$\mathbf{B}(r,t) = B_\theta(r,t)\,\mathbf{e}_\theta + B_0\,\mathbf{e}_z, \tag{1}$$

where B_0 is the constant toroidal magnetic field generated by currents flowing in external field-coils. The poloidal field, $B_\theta(r,t)$, on the other hand, is generated via transformer action by the time variation of the current flowing in the tokamak's primary winding. The current density in the plasma is written $\mathbf{j} = j_z\,\mathbf{e}_z$. Moreover, Ampère's law implies that

$$\mu_0\,j_z(r,t) = \frac{1}{r}\frac{\partial}{\partial r}(r\,B_\theta). \tag{2}$$

The total toroidal current carried by the plasma is

$$I_p(t) = \gamma_s \int_0^a 2\pi\,r\,j_z\,dr = \frac{\gamma_s\,2\pi\,a\,B_\theta(a,t)}{\mu_0}, \tag{3}$$

where

$$\gamma_s = \frac{1+\kappa^2}{2} \tag{4}$$

is an empirical determined factor that specifies the increase in the toroidal current over the cylindrical value in a plasma of vertical elongation κ.[4,15] The plasma safety-factor profile takes the form

$$q(r,t) = \frac{r\,B_0}{R_0\,B_\theta}, \tag{5}$$

4

while the electric field in the plasma is written $\mathbf{E} = E_z\,\mathbf{e}_z$. Faraday's law yields

$$\frac{\partial E_z}{\partial r} = \frac{\partial B_\theta}{\partial t}, \tag{6}$$

while Ohm's law gives

$$E_z = \eta\,j_z, \tag{7}$$

where

$$\eta = \frac{Z\,\ln\Lambda}{1.96\,6\sqrt{2}\,\pi^{3/2}}\,\frac{m_e^{1/2}\,e^2\,c^4\,\mu_0^2}{T_e^{3/2}} \tag{8}$$

is the Spitzer plasma resistivity.[16,17] Here, $T_e(r,t)$ is the electron temperature profile, Z the effective ion charge number, $\ln\Lambda \simeq 15$ the Coulomb logarithm, m_e the electron mass, e the magnitude of the electron charge, c the velocity of light in vacuum, and μ_0 the vacuum permeability. Note that, for the sake of simplicity, we are neglecting both the neoclassical enhancement of the plasma resistivity, as well as the non-inductive bootstrap current.[18] The neoclassical enhancement could most easily be taken into account in our analysis by multiplying Z by the volume-averaged enhancement factor. Finally, it is helpful to define the poloidal magnetic flux, $\psi(r,t)$, where

$$B_\theta = \frac{1}{2\pi\,R_0}\,\frac{\partial\psi}{\partial r}. \tag{9}$$

The electron energy balance equation takes the form[17]

$$\frac{3}{2}\,n_e\,\frac{\partial T_e}{\partial t} - n_e\,\frac{1}{r}\,\frac{\partial}{\partial r}\left(r\,\chi_\perp\,\frac{\partial T_e}{\partial r}\right) = \eta\,j_z^2, \tag{10}$$

where n_e is the electron number density, and $\chi_\perp(r)$ is the electron perpendicular energy diffusivity due to small-scale plasma turbulence. Note that, for the sake of simplicity, we are treating n_e as a spatial and temporal constant. Moreover, we expect $\chi_\perp \sim 1\,\mathrm{m}^2\,\mathrm{s}^{-1}$.[19] Finally, the net power input to the plasma due to ohmic heating is

$$P(t) = \gamma_p\,4\pi^2\,R_0\int_0^a r\,\eta\,j_z^2\,dr, \tag{11}$$

where $\gamma_p = (\gamma_s/\kappa)^2$ is an empirical factor that takes the shaping of the plasma poloidal cross-section into account.[15]

5

C. Fundamental Quantities

Let $\epsilon = a/R_0$ be the inverse aspect-ratio of the plasma, q_a the value of the edge safety-factor at the end of the current ramp, and

$$B_{\theta\, a} = \frac{\epsilon}{q_a}\, B_0 \tag{12}$$

the edge poloidal magnetic field at the end of the current ramp. Suppose that $\chi_\perp(r) = \chi_0\, \hat{\chi}(r)$, where χ_0 is a typical value of the perpendicular energy diffusivity, and $\hat{\chi}(r)$ is dimensionless and of order unity. We can define

$$T_0 = \left[\frac{Z \ln \Lambda}{1.96\, 6\sqrt{2}\, \pi^{3/2}} \frac{m_e^{1/2}\, e^2\, c^4\, B_{\theta\, a}^2}{n_e\, \chi_0} \right]^{2/5} \tag{13}$$

$$= 9.95 \times 10^{-1}\, Z^{2/5}\, \Lambda_{15}^{2/5}\, n_{20}^{-2/5}\, \chi_0^{-2/5}\, B_{\theta\, a}^{4/5}\ [\text{keV}] \tag{14}$$

as the typical electron temperature attained at the end of the current ramp. Here, $\Lambda_{15} = \ln \Lambda/15$ and $n_{20} = n_e/10^{20}$. All other quantities are in SI units. Likewise,

$$\tau_R \equiv \frac{a^2\, \mu_0}{\eta(T_0)} = 4.99 \times 10^1\, a^2\, Z^{-2/5}\, \Lambda_{15}^{-2/5}\, n_{20}^{-3/5}\, \chi_0^{-3/5}\, B_{\theta\, a}^{6/5}\ [\text{s}] \tag{15}$$

is the conventional resistive diffusion time, whereas

$$\tau_c = \frac{a^2}{\chi_0}\ [\text{s}] \tag{16}$$

is the energy confinement time. The plasma poloidal beta is defined

$$\beta_p \equiv \frac{\mu_0\, n_e\, T_0}{B_{\theta\, a}^2} = 2.00 \times 10^{-2}\, Z^{2/5}\, \Lambda_{15}^{2/5}\, n_{20}^{3/5}\, \chi_0^{-2/5}\, B_{\theta\, a}^{-6/5}. \tag{17}$$

Note that

$$\beta_p = \frac{\tau_c}{\tau_R} \tag{18}$$

in an ohmic plasma. The typical plasma current is

$$I_0 = \frac{2\pi\, \gamma_s\, a\, B_{\theta\, a}}{\mu_0} = 5.00\, \gamma_s\, a\, B_{\theta\, a}\ [\text{MA}], \tag{19}$$

whereas typical inductive electric field-strength in the plasma takes the form

$$E_0 = \frac{\beta_p\, \chi_0\, B_{\theta\, a}}{a} = 2.00 \times 10^{-2}\, a^{-1}\, Z^{2/5}\, \Lambda_{15}^{2/5}\, n_{20}^{3/5}\, \chi_0^{3/5}\, B_{\theta\, a}^{-1/5}\ [\text{V m}^{-1}], \tag{20}$$

and the typical ohmic heating power is written

$$P_0 = 4\pi^2 \gamma_p R_0 n_e \chi_0 T_0 = 6.29 \times 10^{-1} \gamma_p R_0 Z^{2/5} \Lambda_{15}^{2/5} n_{20}^{3/5} \chi_0^{3/5} B_{\theta a}^{4/5} \text{ [MW]}. \qquad (21)$$

Finally, the typical poloidal magnetic flux takes the form

$$\psi_0 = 6.28 R_0 a B_{\theta a} \text{ [V s]}. \qquad (22)$$

D.   Runaway Electron Generation

The plasma at the start of the current ramp is cold and resistive. Consequently, driving a current through the discharge requires a comparatively large inductive electric field. In such circumstances, there is a danger of runaway electron generation. Runaway electrons are suprarthermal electrons for which the Coulomb collisional drag due to the bulk plasma is less than the acceleration due to the inductive electric field. Such electrons can acquire energies in excess of 10 MeV, and cause considerable damage if they strike the first wall.

Runaway electron generation is only possible, in theory, when the electric field exceeds the so-called *Connor-Hastie* value,[20]

$$E_c = \frac{\ln \Lambda \, n_e \, e^3}{4\pi \, \epsilon_0^2 \, m_e \, c^2} = 7.65 \times 10^{-2} \Lambda_{15} n_{20} \text{ [V m}^{-1}\text{]}. \qquad (23)$$

Here, ϵ_0 is the vacuum permittivity. However, the criterion $E > E_c$ does not, by itself, guarantee the generation of dangerous quantities of runaway electrons, because, before this can happen, there needs to be a source of suprathermal electrons. One obvious source is from the high-energy tail of the thermal electrons. However, it is well-known that this source does not become effective until the electric field approaches the so-called *Driecer* value,[21]

$$E_D = E_c \frac{m_e \, c^2}{T_e} = E_{D0} \frac{T_e}{T_0}, \qquad (24)$$

where

$$E_{D0} = 3.93 \times 10^1 Z^{-2/5} \Lambda_{15}^{3/5} n_{20}^{7/5} \chi_0^{2/5} B_{\theta a}^{-4/5} \text{ [V m}^{-1}\text{]}. \qquad (25)$$

Note that $E_{D0} \gg E_c$.

In an extensive experimental study of runaway electron generation in the JET tokamak,[22] de Vries et alia (2020) find that JET plasmas invariably satisfy the runaway electron existence

criterion, $E > E_c$, in the early stages of the discharge, but that this does not usually lead to the generation of dangerous quantities of runaway electrons. In fact, de Vries et alia (2020) conclude that $E > 10\,E_c$ is needed before runaway electron generation becomes a problem. This conclusion is consistent with those of earlier experimental studies.[23–25]

E.   Normalization

Let us adopt the following convenient normalization scheme: $r = a\,\hat{r}$, $t = \tau_R\,\hat{t}$, $T_e = T_0\,\hat{T}(\hat{r}, \hat{t})$, $B_\theta = B_{\theta\,a}\,\hat{B}_\theta(\hat{r}, \hat{t})$, $I_p = I_0\,\hat{I}_p(\hat{t})$, $j_z = [B_{\theta\,a}/(\mu_0\,a)]\,\hat{j}$, $E = E_0\,\hat{E}(\hat{r}, \hat{t})$, $E_c = E_0\,\hat{E}_c$, $E_D = E_0\,\hat{E}_D(\hat{r}, \hat{t})$, $E_{D\,0} = E_0\,\hat{E}_{D\,0}$, $P = P_0\,\hat{P}(\hat{t})$, and $\psi = \psi_0\,\hat{\psi}(\hat{r}, \hat{t})$. It follows that

$$\frac{3}{2}\,\beta_p\,\frac{\partial\hat{T}}{\partial\hat{t}} = \frac{\partial^2\hat{T}}{\partial\hat{r}^2} + \frac{1}{\hat{r}}\,\frac{\partial\hat{T}}{\partial\hat{r}} + \frac{d\ln\hat{\chi}}{d\hat{r}}\,\frac{\partial\hat{T}}{\partial\hat{r}} + \frac{\hat{E}^2\,\hat{T}^{3/2}}{\hat{\chi}}, \tag{26}$$

$$\frac{\partial\hat{B}_\theta}{\partial\hat{r}} + \frac{\hat{B}_\theta}{\hat{r}} = \hat{E}\,\hat{T}^{3/2}, \tag{27}$$

$$\frac{\partial\hat{B}_\theta}{\partial\hat{t}} = \frac{\partial\hat{E}}{\partial\hat{r}}, \tag{28}$$

as well as

$$\frac{q}{q_a} = \frac{\hat{r}}{\hat{B}_\theta}, \tag{29}$$

$$\hat{I}_p(\hat{r}, \hat{t}) = \hat{r}\,\hat{B}_\theta(\hat{r}, \hat{t}), \tag{30}$$

$$\hat{B}_\theta = \frac{\partial\hat{\psi}}{\partial\hat{r}}, \tag{31}$$

$$\hat{E}_D = \hat{E}_{D\,0}\,\hat{T}^{-1}, \tag{32}$$

Here, $\hat{I}_p(\hat{r}, \hat{t})$ is the normalized toroidal plasma current contained within normalized minor radius $\hat{r}$. Equation (28) can be integrated to give

$$\hat{E}(\hat{r}, \hat{t}) = \frac{\partial\hat{\psi}}{\partial\hat{t}} = \mathcal{E}(\hat{t}) + \int_0^{\hat{r}} \frac{\partial\hat{B}_\theta}{\partial\hat{t}}\,d\hat{r}', \tag{33}$$

where use has been made of Eq. (31). It follows that

$$\mathcal{E}(\hat{t}) = \frac{\partial\hat{\psi}(0, \hat{t})}{\partial\hat{t}}. \tag{34}$$

Finally, it can be shown that

$$\hat{E}_c = 3.82 \, a \, Z^{-2/5} \, \Lambda_{15}^{3/5} \, n_{20}^{2/5} \, \chi_0^{-3/5} \, B_{\theta\,a}^{1/5}, \tag{35}$$

$$\hat{E}_{D0} = 1.96 \times 10^3 \, Z^{-4/5} \, \Lambda_{15}^{3/5} \, n_{20}^{4/5} \, \chi_0^{-1/5} \, B_{\theta\,a}^{-3/5}. \tag{36}$$

F.   Approximations

In order to facilitate our analysis, we shall make two main approximations. Our first approximation is to neglect the term involving β_p in Eq. (26). This approximation is warranted because, as is clear from Eq. (17), β_p is much less than unity in conventional ohmic tokamak plasmas. (See also Table II.) As is apparent from Eq. (18), β_p is much less than unity because the energy confinement time is much less than the resistive diffusion time in ohmic plasmas. The neglect of the term in question implies that, during the current ramp, the temperature profile remains in a quasi-equilibrium state in which the energy per unit time that flows across the plasma boundary, and is presumably absorbed by the limiter, matches the ohmic heating power. Under these circumstances, the normalized ohmic heating power is written

$$\hat{P}(\hat{t}) = -\left(\hat{\chi} \, \hat{r} \, \frac{\partial \hat{T}}{\partial \hat{r}} \right)_{\hat{r}=1}. \tag{37}$$

Our second approximation is to neglect the second term on the extreme right-hand side of Eq. (33). The neglect of the term in question implies that the inductive electric field is *uniform* within the plasma. Of course, this is the usual situation during the current flat-top phase of a tokamak discharge. However, it is possible for the electric field to be spatially uniform during a current ramp, provided that the current is not ramped up or down too rapidly. Indeed, the criterion that must be satisfied is

$$\mathcal{E} > \left| \int_0^1 \frac{\partial \hat{B}_\theta}{\partial \hat{t}} \, d\hat{r}' \right|. \tag{38}$$

During the ramp-up phase, if the toroidal current is ramped up sufficiently rapidly that the criterion (38) is not satisfied then the electric field in the outer regions of the plasma becomes greater than that in the core, leading to a broadening of the current profile. However, a

broad current profile implies a low internal plasma inductance, and low-inductance plasmas are prone to destructive ideal-kink instabilities.[12,14] If the current is ramped-up extremely rapidly then the current profile becomes hollow, giving rise to minor disruption events that rapidly relax the current profile toward a more peaked profile, but also occasionally trigger major disruptions.[23] During the ramp-down phase, on the other hand, if the current is ramped down sufficiently rapidly that the criterion (38) is not satisfied then the electric field in the outer regions of the plasma becomes less than that in the core, leading to a peaking of the current profile. However, plasmas with strongly peaked current profiles are prone to tearing instabilities that can lead to major disruptions.[12,14] Thus, the criterion (38) is a necessary one for the completely safe operation of a tokamak during the current ramp-up and ramp-down phases.

Our two approximations lead to the following equations:

$$\frac{\partial^2 \hat{T}}{\partial \hat{r}^2} + \frac{1}{\hat{r}} \frac{\partial \hat{T}}{\partial \hat{r}} + \frac{d \ln \hat{\chi}}{d \hat{r}} \frac{\partial \hat{T}}{\partial \hat{r}} + \frac{\mathcal{E}^2 \, \hat{T}^{3/2}}{\hat{\chi}} = 0, \tag{39}$$

$$\frac{\partial \hat{B}_\theta}{\partial \hat{r}} + \frac{\hat{B}_\theta}{\hat{r}} = \mathcal{E} \, \hat{T}^{3/2}. \tag{40}$$

Note that $\mathcal{E}(t)$ can be adjusted by changing the time derivative of the current flowing in the central solenoid. Furthermore, tokamaks invariably possess a feedback system that automatically alters the instantaneous value of $\mathcal{E}(t)$ in such a manner as to produce a prescribed plasma current waveform, $I_p(t)$.

G. Rescaling

Suppose that the instantaneous minor radius of the plasma is $\delta(\hat{t}) \, a$. In other words, suppose that the limiter is situated at $\hat{r} = \delta$. Let $x = \hat{r}/\delta$, and let

$$\hat{T}(\hat{r}, \hat{t}) = \frac{\lambda^2}{(\delta \, \mathcal{E})^4} \, \bar{T}(x). \tag{41}$$

Equation (39) transforms to give

$$\frac{d^2 \bar{T}}{dx^2} + \frac{1}{x} \frac{d\bar{T}}{dx} + \frac{d \ln \hat{\chi}}{dx} \frac{d\bar{T}}{dx} + \frac{\lambda \, \bar{T}^{3/2}}{\hat{\chi}} = 0. \tag{42}$$

Appropriate boundary conditions are

$$\bar{T}(0) = 1, \tag{43}$$

$$\frac{d\bar{T}(0)}{dx} = 0, \tag{44}$$

$$\bar{T}(1) = 0. \tag{45}$$

The parameter λ must be adjusted until Eq. (45) is satisfied. Clearly, the determination of the normalized electron temperature profile, $\bar{T}(x)$, involves the solution of a nonlinear eigenvalue equation, (42), where λ plays the role of the eigenvalue. Of course, the electron temperature is not zero at the plasma boundary, but is, instead, determined by sheath physics at the plasma/limiter interface. However, we expect the edge temperature to be much lower than that in the plasma interior, which justifies the approximation $\bar{T}(1) = 0$.

Let

$$\hat{B}_\theta(\hat{r}, \hat{t}) = \frac{\lambda^3}{(\delta\,\mathcal{E})^5}\,\bar{B}_\theta(x). \tag{46}$$

Equation (40) yields

$$\frac{d\bar{B}_\theta}{dx} + \frac{\bar{B}_\theta}{x} = \bar{T}^{3/2}, \tag{47}$$

which must be solved subject to the boundary condition

$$\frac{d\bar{B}(0)}{dx} = 0. \tag{48}$$

Let

$$q(\hat{r}, \hat{t}) = \frac{q_a\,\delta\,(\delta\,\mathcal{E})^5}{\lambda^3}\,\bar{q}(x). \tag{49}$$

Equation (29) gives

$$\bar{q}(x) = \frac{x}{\bar{B}_\theta(x)}. \tag{50}$$

Note that

$$\bar{q}(0) = 2. \tag{51}$$

According to Eq. (30), the net normalized toroidal current flowing in the plasma is

$$\hat{I}_p(\hat{t}) \equiv \hat{I}_p(\delta, \hat{t}) = \frac{\lambda^3\,\delta}{(\delta\,\mathcal{E})^5}\,\bar{B}_\theta(1). \tag{52}$$

11

Equation (37) implies that the normalized ohmic heating power is

$$\hat{P}(\hat{t}) = \frac{\lambda^2}{(\delta\,\mathcal{E})^4}\,\zeta, \tag{53}$$

where

$$\zeta = -\left(\hat{\chi}\,x\,\frac{d\bar{T}}{dx}\right)_{x=1}. \tag{54}$$

According to Eq. (31), the total normalized poloidal magnetic flux contained between the magnetic axis and the plasma boundary is

$$\hat{\psi}_{\text{tot}}(\hat{t}) = \frac{\lambda^3\,\delta}{(\delta\,\mathcal{E})^5}\int_0^1 \bar{B}_\theta\,dx. \tag{55}$$

Finally, the criterion (38) becomes

$$\mathcal{E} > \delta\left|\frac{d}{d\hat{t}}\left[\frac{\lambda^3}{(\delta\,\mathcal{E})^5}\right]\right|\int_0^1 \bar{B}(x)\,dx. \tag{56}$$

Note that we have imposed the criterion at $r = \delta\,a$, rather than $r = a$, because it only needs to be satisfied within the plasma.

IV. CURRENT RAMP SCENARIOS

A. Current Ramp-Up

1. Current Waveform

Suppose that the current ramp-up lasts from $t = 0$ to $t = t_{\text{ramp}}$. Suppose that, during the ramp-up, the current flowing in the central solenoid is adjusted such that the normalized plasma current increases *linearly* in time:

$$\hat{I}_p(\hat{t}) = \frac{\hat{t}}{\hat{t}_{\text{ramp}}}, \tag{57}$$

where $\hat{t}_{\text{ramp}} = t_{\text{ramp}}/\tau_R$. For the sake of simplicity, we shall assume that the plasma elongation, κ, is constant in time.

2. Initial Stage

Suppose that, during the initial stage of the ramp-up, which lasts from $t = 0$ to $t = t_{\text{pre}}$, where $t_{\text{pre}} \ll t_{\text{ramp}}$, the safety-factor at the plasma boundary is allowed to decrease from an initial very large value to its final value, q_a, in such a manner that

$$q(x, \hat{t}) = q_a \left(\frac{\hat{t}_{\text{pre}}}{\hat{t}} \right) \frac{\bar{q}(x)}{\bar{q}(1)}, \tag{58}$$

where $\hat{t}_{\text{pre}} = t_{\text{pre}}/\tau_R$. Here, q_a is chosen such that $q(0) = 1$ at the end of the initial stage. We make this choice because the sawtooth oscillation effectively prevents the central safety-factor from falling significantly below unity.[19] It follows that

$$q_a = \frac{1}{2\,\bar{B}_\theta(1)}. \tag{59}$$

Equations (57) and (58) allow us to determine all other quantities in the initial stage of the ramp-up. We obtain

$$\delta = \left(\frac{\hat{t}_{\text{pre}}}{\hat{t}_{\text{ramp}}} \right)^{1/2}, \tag{60}$$

which implies that the plasma minor radius takes a relatively small constant value during the first stage of the ramp-up. Furthermore,

$$\hat{T}(x, \hat{t}) = T_{\text{ramp}} \left(\frac{\hat{t}_{\text{pre}}}{\hat{t}_{\text{ramp}}} \right)^{2/5} \left(\frac{\hat{t}}{\hat{t}_{\text{pre}}} \right)^{4/5} \bar{T}(x), \tag{61}$$

$$\hat{B}_\theta(x, \hat{t}) = \left(\frac{\hat{t}_{\text{pre}}}{\hat{t}_{\text{ramp}}} \right)^{1/2} \left(\frac{\hat{t}}{\hat{t}_{\text{pre}}} \right) \frac{\bar{B}_\theta(x)}{\bar{B}_\theta(1)}, \tag{62}$$

$$\mathcal{E}(\hat{t}) = \mathcal{E}_{\text{ramp}} \left(\frac{\hat{t}_{\text{pre}}}{\hat{t}_{\text{ramp}}} \right)^{-3/5} \left(\frac{\hat{t}}{\hat{t}_{\text{pre}}} \right)^{-1/5}, \tag{63}$$

$$\hat{P}(\hat{t}) = P_{\text{ramp}} \left(\frac{\hat{t}_{\text{pre}}}{\hat{t}_{\text{ramp}}} \right)^{2/5} \left(\frac{\hat{t}}{\hat{t}_{\text{pre}}} \right)^{4/5}, \tag{64}$$

$$\hat{\psi}_{\text{tot}}(\hat{t}) = \left(\frac{\hat{t}}{\hat{t}_{\text{ramp}}} \right) \int_0^1 \frac{\bar{B}_\theta(x)}{\bar{B}_\theta(1)}\, dx, \tag{65}$$

where

$$T_{\text{ramp}} = \lambda^{-2/5} \left[\bar{B}_\theta(1) \right]^{-4/5}, \tag{66}$$

13

$$\mathcal{E}_{\text{ramp}} = \lambda^{3/5} \, [\bar{B}_\theta(1)]^{1/5}, \tag{67}$$

$$P_{\text{ramp}} = \zeta \, T_{\text{ramp}}. \tag{68}$$

Finally, the criterion (56) yields

$$\hat{t}_{\text{ramp}} > \left(\frac{\hat{t}_{\text{pre}}}{\hat{t}_{\text{ramp}}}\right)^{3/5} \left(\frac{\hat{t}}{\hat{t}_{\text{pre}}}\right)^{1/5} \mathcal{E}_{\text{ramp}}^{-1} \int_0^1 \frac{\bar{B}_\theta(x)}{\bar{B}_\theta(1)} \, dx, \tag{69}$$

which does indeed constitute a limitation on the maximum current ramp rate.

3. Main Stage

In the main stage of the current ramp-up, the plasma current still increases linearly in time according to Eq. (57), but the edge safety-factor value is held constant in such a manner that

$$q(x, \hat{t}) = q_a \, \frac{\bar{q}(x)}{\bar{q}(1)}. \tag{70}$$

As before, Eqs. (57) and (70) allow us to determine all other quantities in the main stage of the ramp-up. We find that

$$\delta = \left(\frac{\hat{t}}{\hat{t}_{\text{ramp}}}\right)^{1/2}, \tag{71}$$

$$\hat{T}(x, \hat{t}) = T_{\text{ramp}} \left(\frac{\hat{t}}{\hat{t}_{\text{ramp}}}\right)^{2/5} \bar{T}(x), \tag{72}$$

$$\hat{B}_\theta(x, \hat{t}) = \left(\frac{\hat{t}}{\hat{t}_{\text{ramp}}}\right)^{1/2} \frac{\bar{B}_\theta(x)}{\bar{B}_\theta(1)}, \tag{73}$$

$$\mathcal{E}(\hat{t}) = \mathcal{E}_{\text{ramp}} \left(\frac{\hat{t}}{\hat{t}_{\text{ramp}}}\right)^{-3/5}, \tag{74}$$

$$\hat{P}(\hat{t}) = P_{\text{ramp}} \left(\frac{\hat{t}}{\hat{t}_{\text{ramp}}}\right)^{2/5}, \tag{75}$$

$$\hat{\psi}_{\text{tot}}(\hat{t}) = \left(\frac{\hat{t}}{\hat{t}_{\text{ramp}}}\right) \int_0^1 \frac{\bar{B}_\theta(x)}{\bar{B}_\theta(1)} \, dx. \tag{76}$$

It is clear from Eq. (71) that, in order to keep the edge safety-factor constant, while the plasma current increases in time, it is necessary for the minor radius of the plasma to also increase in time.

14

The criterion (56) yields

$$\hat{t}_{\text{ramp}} > \left(\frac{\hat{t}}{\hat{t}_{\text{ramp}}}\right)^{3/5} \frac{1}{2\,\mathcal{E}_{\text{ramp}}} \int_0^1 \frac{\bar{B}_\theta(x)}{\bar{B}_\theta(1)}\,dx, \qquad (77)$$

Now, if this criterion is satisfied at the end of the current ramp then it is satisfied at all times in the main current ramp, and the criterion (69) is also satisfied at all times in the initial stage of the current ramp. We conclude that the criterion (56) is satisfied at all times in the current ramp provided

$$t_{\text{ramp}} > \tau_{\text{min}}, \qquad (78)$$

where

$$\tau_{\text{min}} = \frac{\tau_R}{2\,\mathcal{E}_{\text{ramp}}} \int_0^1 \frac{\bar{B}_\theta(x)}{\bar{B}_\theta(1)}\,dx, \qquad (79)$$

Clearly, τ_{min} represents the minimum possible completely safe current ramp-up timescale.

B. Current Ramp-Down

Suppose that the current ramp-down lasts from $t = 0$ to $t = t_{\text{ramp}}$. Suppose that, during the ramp-down, the normalized plasma current decreases linearly in time:

$$\hat{I}_p(\hat{t}) = \frac{\hat{t}_{\text{ramp}} - \hat{t}}{\hat{t}_{\text{ramp}}}. \qquad (80)$$

In the main stage of the ramp-down, the edge safety-factor is held constant, so that Eq. (70) is valid. In the final stage of the ramp-down, which lasts from $t = t_{\text{ramp}} - t_{\text{pre}}$ to $t = t_{\text{ramp}}$, the edge safety-factor increases in such a manner that

$$q(x, \hat{t}) = q_a\left(\frac{\hat{t}_{\text{pre}}}{\hat{t}_{\text{ramp}} - \hat{t}}\right)\frac{\bar{q}(x)}{\bar{q}(1)}. \qquad (81)$$

The time variation of other quantities during the main stage of ramp-down can be obtained by making the transformation $\hat{t} \to \hat{t}_{\text{ramp}} - \hat{t}$ in the relevant formulae given in Sect. IV A 3. Likewise, the time variation of other quantities during the final stage of the ramp down are obtained be making the same transformation in the relevant formulae given in Sect. IV A 2. Clearly, the current ramp-down is the mirror image in time of the current ramp-up. In particular, the minimum completely safe current ramp-down timescale, τ_{min}, is specified in Eq. (79).

15

V.   RESULTS

A.   Plasma Equilibrium

Let our normalized perpendicular energy diffusivity profile take the form

$$\hat{\chi}(x) = f(\alpha)\,(1 + x^2)^\alpha, \tag{82}$$

where

$$f(\alpha) = \frac{1 + \alpha}{2^{1+\alpha} - 1}. \tag{83}$$

Note that $\int_0^1 \hat{\chi}(x)\,dx / \int_0^1 x\,dx = 1$, which ensures that χ_0 is the volume averaged perpendicular diffusivity, in accordance with our earlier assumption.

Figure 2 shows various equilibrium quantities plotted as a function of α. As α increases, which implies that the diffusivity at the plasma boundary becomes larger than that in the core, the equilibrium current profile becomes more peaked. This is clear from the figure because both the edge safety-factor value, q_a, and the normalized internal plasma inductance,[14]

$$l_i = \frac{2}{\bar{B}_\theta^2(1)} \int_0^1 \bar{B}_\theta^2(x)\,x\,dx, \tag{84}$$

increase with increasing α. (A peaked current profile is associated with large q_a/q_0 and l_i values, and vice versa.[12,19]) The peaking of the current profile also causes a decrease in the normalized central electric field, $\mathcal{E}_{\mathrm{ramp}}$, with increasing α. Note that $P_{\mathrm{ramp}} = \mathcal{E}_{\mathrm{ramp}}$ for the set of equilibria in question. Finally, the minimum safe current ramp timescale, τ_{min}, is an increasing function of α.

For the sake of simplicity, let us consider the case $\alpha = 0$, in which the perpendicular diffusivity is uniform within the plasma. In this situation, we find that $\lambda = 7.01$, $q_a = 3.30$, $l_i = 1.25$, $T_{\mathrm{ramp}} = 2.08$, $\mathcal{E}_{\mathrm{ramp}} = P_{\mathrm{ramp}} = 2.21$, and $\tau_{\mathrm{min}}/\tau_R = 0.214$. Figure 3 shows the corresponding normalized electron temperature and current profiles, as well as the safety-factor profile. It can be seen that the current profile is fairly broad. Nevertheless, the equilibrium lies in the stable region of the conventional q_a–l_i diagram. (See Fig. 4 of Ref. 14.) Note that, due to profile effects, the minimum ramp timescale, τ_{min}, is about one fifth of the conventional resistive diffusion timescale, τ_R.

B. Simulated Current Ramp-Up

In this section, we shall describe simulated current ramp-ups made using our model for the JET, SPARC, and ITER tokamaks. The machine parameters for these tokamaks are given in Table I. The simulations are made assuming that $\chi_0 = 1 \, \mathrm{m \, s^{-1}}$, $\ln \Lambda = 15$, $Z = 2$, $t_{\mathrm{pre}} = 0.05 \, t_{\mathrm{ramp}}$, and $t_{\mathrm{ramp}} = \tau_{\mathrm{min}}$. Note that the current ramp time in these simulations takes its minimum completely safe value, according to our model.

Figure 4 shows a simulated current ramp-up for JET. Some of the characteristic parameters for this ramp-up are listed in Table II. It can be seen that the toroidal plasma current in JET can be safely ramped up to about 4.3 MA in about 4.2 seconds. This prediction accords well with operational experience in JET. (See Fig. 1 of Ref. 26.) Note that, as reported by de Vries et alia (2020),[22] the inductive electric field exceeds the Connor-Hastie field during the current ramp-up. However, the electric field only exceeds de Vries et alia's (2020) empirical runaway electron generation threshold, which is ten times the Connor-Hastie field,[22] in the very early stages of the current ramp-up. Note that the threshold is exceeded, not because the current ramp rate is too large, but rather because the plasma is very cold and resistive in the early stages of the ramp-up. One obvious solution to runaway electron problems in the early stages of a current ramp-up is to apply small amounts of electron cyclotron wave heating in order to slightly raise the electron temperature. The inductive electric field is slightly above the Connor-Hastie value at the end of the current ramp-up, but we would expect the field to fall as soon as the main external heating is applied. Hence, the inductive electric field should be well below the Connor-Hastie value throughout most of the current flat-top. Note that the inductive electric field is very much less than the Dreicer field throughout the current ramp-up, as is also the case for our SPARC and ITER simulations.

Figure 5 shows a simulated current ramp-up for SPARC. Some of the characteristic parameters for this ramp-up are listed in Table II. It can be seen that the toroidal plasma current in SPARC can be safely ramped up to about 9.5 MA in about 2.0 seconds. This maximum safe ramp-rate is actually greater than the ramp-rate in the SPARC design.[4] Note that the inductive electric field, $\mathcal{E}$, exceeds the Connor-Hastie field, E_c, during the current ramp-up. However, the ratio $\mathcal{E}/E_c$ for SPARC, shown in Fig. 5, is less than that the corre-

sponding ratio for JET, shown in Fig. 4. In other words, if JET was capable of operating without dangerous levels of runaway electron generation during the current ramp-up, as reported by Vries et alia (2020),[22] then SPARC should certainly also be capable of operating without runaway electron problems.

Finally, Fig. 6 shows a simulated current ramp-up for ITER. Some of the characteristic parameters for this ramp-up are listed in Table II. It can be seen that the toroidal plasma current in ITER can be safely ramped up to about 14.0 MA in about 14.7 seconds. This maximum safe ramp-rate is consistent with the series of equilibria shown in Fig. 1 of Ref. 9, and is much greater than the 15 MA in 60 s ramp-down rate envisioned by de Vries et alia (2018).[2] Note that the inductive electric field, $\mathcal{E}$, exceeds the Connor-Hastie field, E_c, during the first third of the current ramp-up. However, the ratio $\mathcal{E}/E_c$ for ITER, shown in Fig. 6, is very much less than that the corresponding ratio for JET, shown in Fig. 4. As before, we conclude that if JET was capable of operating without dangerous levels of runaway electron generation during the current ramp-up, then ITER should certainly also be capable operating without runaway electron problems.

VI. SUMMARY

A simple model of the ramp-up and ramp-down of the toroidal current in a tokamak plasma is developed. Faraday's law of electric induction is found to limit how rapidly the current can be safety ramped up or down. We estimate that the minimum completely safe ramp-up/down times for the JET, SPARC, and ITER tokamaks are 4.2, 2.0, and 14.7 seconds, respectively. The JET ramp time is in accordance with operational experience. The SPARC and ITER minimum safe ramp times are less than the ramp times in the respective designs. Hence, there is no indication that the design ramp times are infeasible, as was recently suggested by Boozer.[1] We also find that the typical ratios of the inductive electric field to the Connor-Hastie field in SPARC and ITER are less than those in JET. Thus, the fact that the JET tokamak was able to operate successfully without encountering runaway electron problems during current ramps suggests that the future SPARC and ITER tokamaks should certainly be able to avoid such problems.

18

DATA AVAILABILITY STATEMENT

The digital data used in the figures in this paper can be obtained from the author upon reasonable request.

[1] A.H. Boozer, arXiv preprint arXiv:2507.05456 (2025).

[2] P.C. de Vries, T.C. Luce, Y.S. Bae, S. Gerhardt, X. Gong, Y. Gribov, D. Humphreys, A. Kavin, R.R. Khayrutdinov, C. Kessel, et al., Nucl. Fusion **58** 026019 (2018).

[3] A.H. Boozer, Nucl. Fusion **61**, 054004 (2021).

[4] A.J. Creely, M.J. Greenwald, S.B. Ballinger, D. Brunner, J. Canik, J. Dooly, T. Fülop, D.T. Garnier, R. Granetz, et al., J. Plasma Phys. **86**, 865860502 (2020).

[5] T. Casper, Y. Gribov, A. Kavin, V. Lukash, R.R. Khayrutdinov, H. Fujieda and C. Kessel, Nucl. Fusion **54**, 013005 (2014).

[6] S.H. Kim, R.H. Bulmer, D.J. Campbell, T.A. Casper, L.L. LoDestro, W.H. Meyer, L.D. Pearlstein and J.A. Snipes, Nucl. Fusion **56**, 126002 (2016).

[7] S.C. Jardin, N. Pomphrey and J. Delucia, J. Comput. Phys. **66**, 481 (1986).

[8] J.B. Lister, A. Portone and Y. Gribov, IEEE Control Systems Magazine **26**, no. 2, 79 (2006).

[9] G. Federici, O. Zolotukhin, M. Kobayashi, A. Loarte, G. Strohmayer, A. Tanga, A. Portone, L. Horton, Y. Feng, F. Sardei, et al., J. Nucl. Materials **363**, 346 (2007).

[10] G.L. Jackson, P.A. Politzer, D.A. Humphreys, T.A. Casper, A.W. Hyatt, J.A. Leuer, J. Lohr, T.C. Luce, M.A. Van Zeeland and J.H. Yu, Phys. Plasmas **17**, 056116 (2010).

[11] P.A. Politzer, G.L. Jackson, D.A. Humphreys, T.C. Luce, A.W. Hyatt and J.A. Leuer, Nucl. Fusion **50**, 035011 (2010).

[12] J.A. Wesson, Nucl. Fusion **18**, 87 (1987).

[13] R.S. Granetz, I.J. Hutchinson and D.O. Overskei, Nucl. Fusion **19**, 1587 (1979).

[14] C.Z. Cheng, H.P. Furth and A.H. Boozer, Plasma Phys. Control. Fusion **29**, 351 (1987).

[15] N.A. Uckan and the ITER Physics Group, *ITER Physics Design Guidelines: 1989*, (IAEA, Vienna, 1990).

[16] L. Spitzer, Jr., *Physics of Fully Ionized Gases* (Interscience, New York NY, 1956).

[17] R. Fitzpatrick, *Plasma Physics: An Introduction*, 2nd ed., (CRC, Boca Raton FL, 2023).

[18] R. Fitzpatrick, *Tearing Mode Dynamics in Tokamak Plasmas*, (IOP, Bristol UK, 2023).

[19] J.A. Wesson, *Tokamaks*, 4th ed., (Oxford, Oxford UK, 2011).

[20] J.W. Connor and R.J. Hastie, Nucl. Fusion **15**, 415 (1975).

[21] H. Dreicer, Phys. Rev. **115**, 238 (1959).

[22] P.C. de Vries, Y. Gribov, J.R. Martin-Solis, A.B. Mineev, J. Sinha, A.C.C. Sips, V. Kiptily, A. Loarte and JET Contributors, Plasma Phys. Control. Fusion **62**, 125014 (2020).

[23] R. Granetz, B. Eposito, J.H. Kim, R. Koslowski, M. Lehnen, J.R. Martin-Solis, C. Paz-Solden, T. Rhee, J.C. Wesley and L. Zheng, Phys. Plasmas **21**, 072506 (2014).

[24] C. Paz-Solden, N.W. Eidietis, R. Granetz, E.M. Hollmann, R.A. Moyer, J.C. Wesley, J. Zhang, M.E. Austin, N.A. Crocker, A. Wingen and Y. Zhu, Phys. Plasmas **21**, 022514 (2014).

[25] Z. Popovic, B. Esposito, J.R. Martin-Solis, W. Bin, P. Buratti, D. Carnevale, F. Causa, M. Gospodarczyk, D. Marocco, G. Ramogida and M. Riva, Phys. Plasmas **23**, 122501 (2016).

[26] I. Voitsekhovitch, A.C.C. Sips, B. Alper, M. Beurskens, I. Coffey, J. Conboy, T. Gerbaud, C. Giroud1, T. Johnson, F. Köch, et al, Plasma Phys. Control. Fusion **52** 105011 (2010).

[27] Z.S. Hartwig and Y.A. Podpaly, *Magnetic Fusion Energy Formulary*, (MIT, Cambridge MA, 2011).

[28] ITER Physics Basis Editors, et al., Nucl. Fusion **39** 2137 (1999).

Machine	R_0(m)	a(m)	B_0(T)	$n_e(10^{20}\,\mathrm{m}^{-3})$	κ
JET	2.96	0.96	3.45	0.3	1.7
SPARC	1.85	0.57	12.2	2.0	1.97
ITER	6.2	2.0	5.3	1.0	1.85

TABLE I. Machine parameters for the JET, SPARC, and ITER tokamaks. The JET parameters come from Ref. 27. The SPARC and ITER parameters are taken from Tables 1 and 2 of Ref. 4, as well as Table 1 of Ref. 28. Here, R_0 is the major radius, a the minor radius, B_0 the toroidal magnetic field-strength, n_e the electron number density, and κ the vertical elongation.

Machine	I_p(MA)	P(MW)	T_c(keV)	β_p	$\mathcal{E}(\mathrm{V\,m}^{-1})$	$E_c(\mathrm{V\,m}^{-1})$	$E_D(\mathrm{V\,m}^{-1})$	τ_{min}(s)
JET	4.26	2.34	1.86	0.0470	0.0336	0.0229	13.1	4.19
SPARC	9.53	12.7	2.29	0.0343	0.151	0.153	70.9	2.02
ITER	14.0	14.4	1.61	0.0583	0.0332	0.0765	50.4	14.7

TABLE II. Plasma parameters at end of current ramp for the JET, SPARC, and ITER tokamaks. Here, I_p is the toroidal plasma current, P the ohmic heating power, T_c the central electron temperature, β_p the central poloidal beta, $\mathcal{E}$ the inductive electric field, E_c the Connor-Hastie field, and E_D the central Dreicer field. Finally, τ_{min} is the minimum safe current ramp timescale.
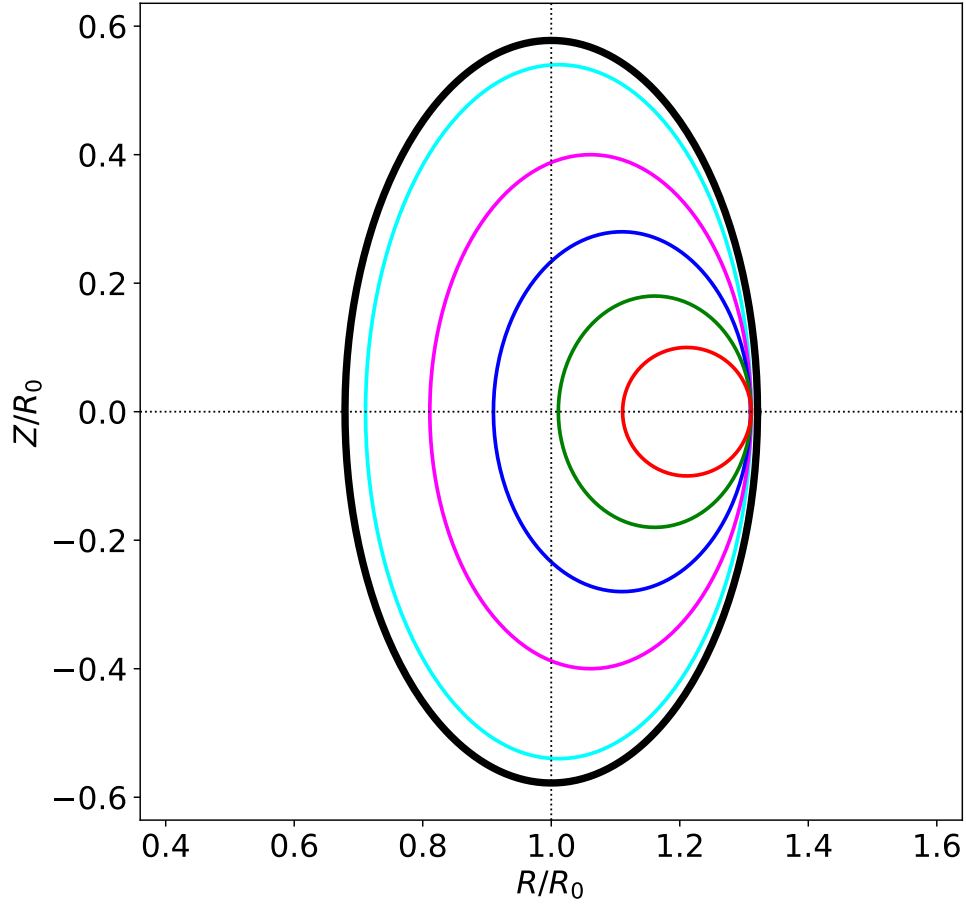
FIG. 1. A cartoon showing the poloidal cross-section of a conventional tokamak during a current ramp-up. The black curve represents the first wall. The red, green, blue, magenta, and cyan curves show, in order of increasing time, the plasma boundary at various stages of the current ramp-up. Here, R, ϕ, Z are conventional cylindrical coordinates that are co-axial with the plasma torus.
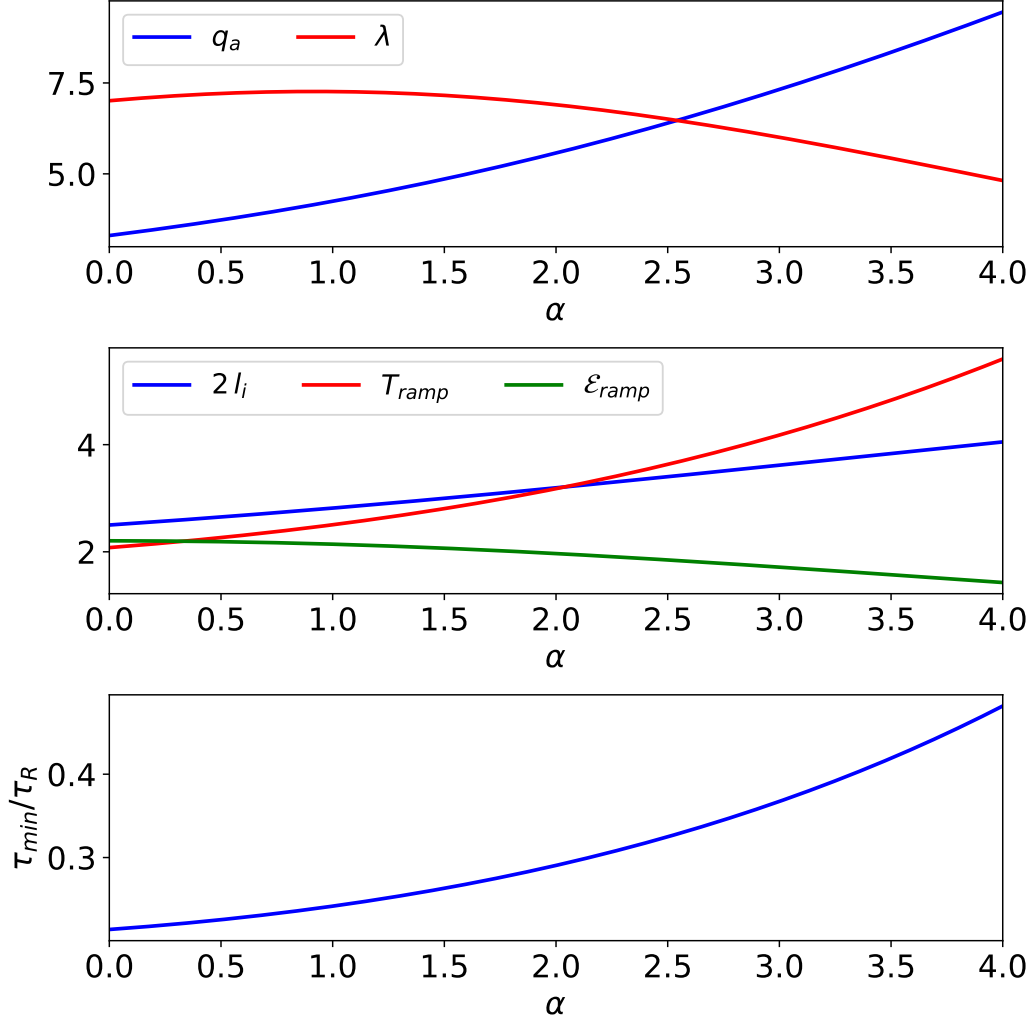
FIG. 2. Various equilibrium quantities calculated as functions of the diffusivity profile parameter, α. The top panel shows the eigenvalue, λ, and the edge safety-factor value, q_a. The middle panel shows the normalized plasma self-inductance, l_i, the normalized central electron temperature, T_{ramp}, and the normalized inductive electric field, $\mathcal{E}_{\mathrm{ramp}}$. The lower panel shows the ratio of the minimum safe current ramp timescale, τ_{min}, to the resistive diffusion timescale, τ_R.
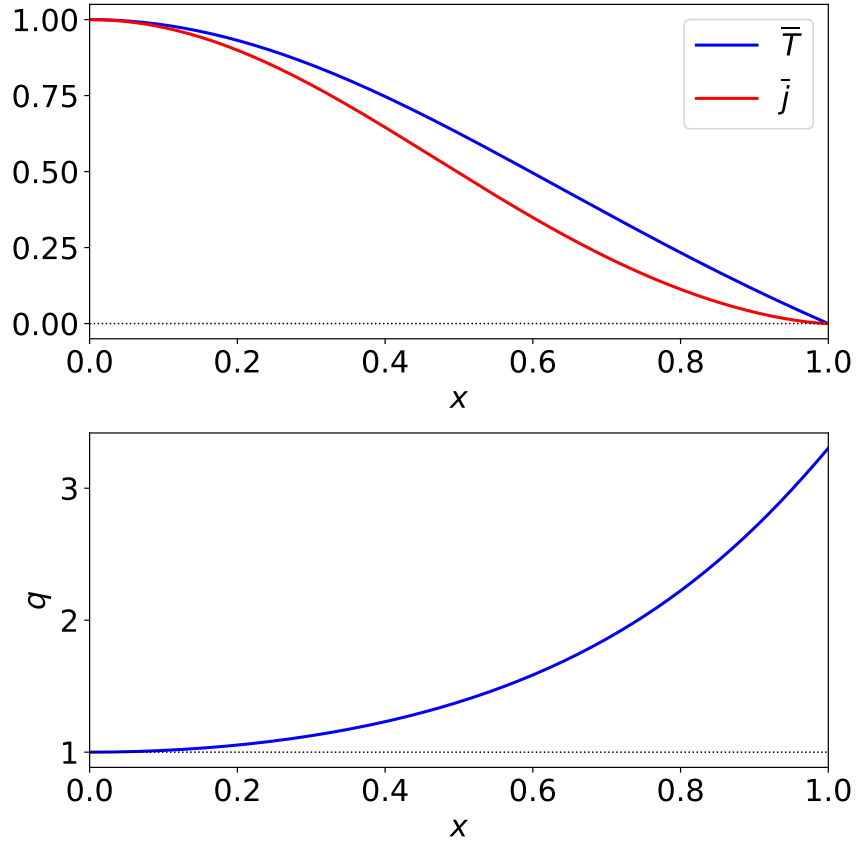
FIG. 3. Equilibrium profiles calculated as functions of the normalized minor radius, x, for $\alpha = 0$. The top panel shows the normalized electron temperature profile, $\bar{T}(x)$, and the normalized current profile, $\bar{j}(x) = \bar{T}^{3/2}$. The bottom panel shows the safety-factor profile, $q(x) = q_a\,\bar{q}(x)$.
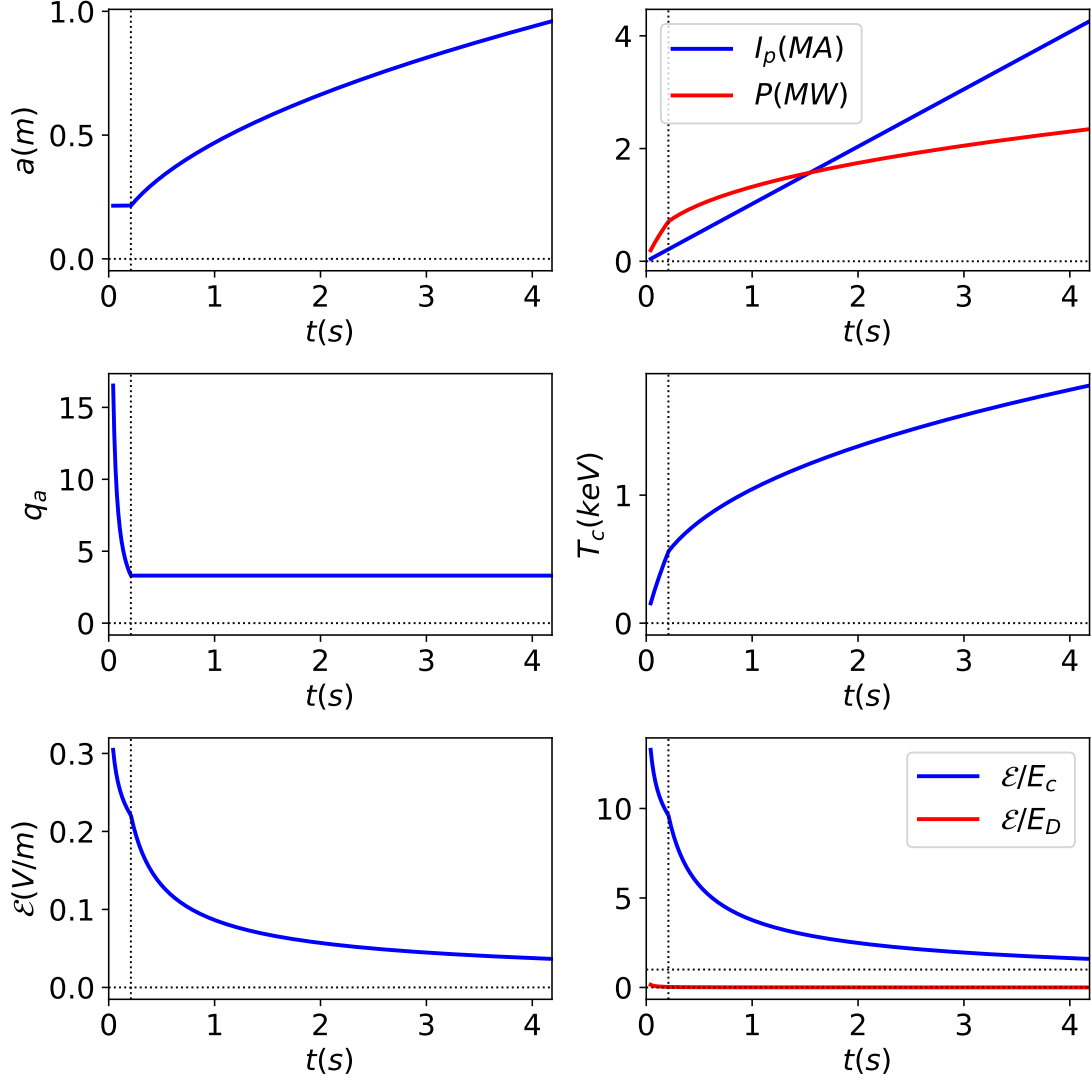
FIG. 4. Simulated current ramp-up for the JET tokamak. Here, a is the minor radius of the plasma, I_p the toroidal plasma current, P the ohmic power, q_a the edge safety-factor, T_c the central electron temperature, $\mathcal{E}$ the inductive electric field, E_c the Connor-Hastie field, and E_D the central Dreicer field.
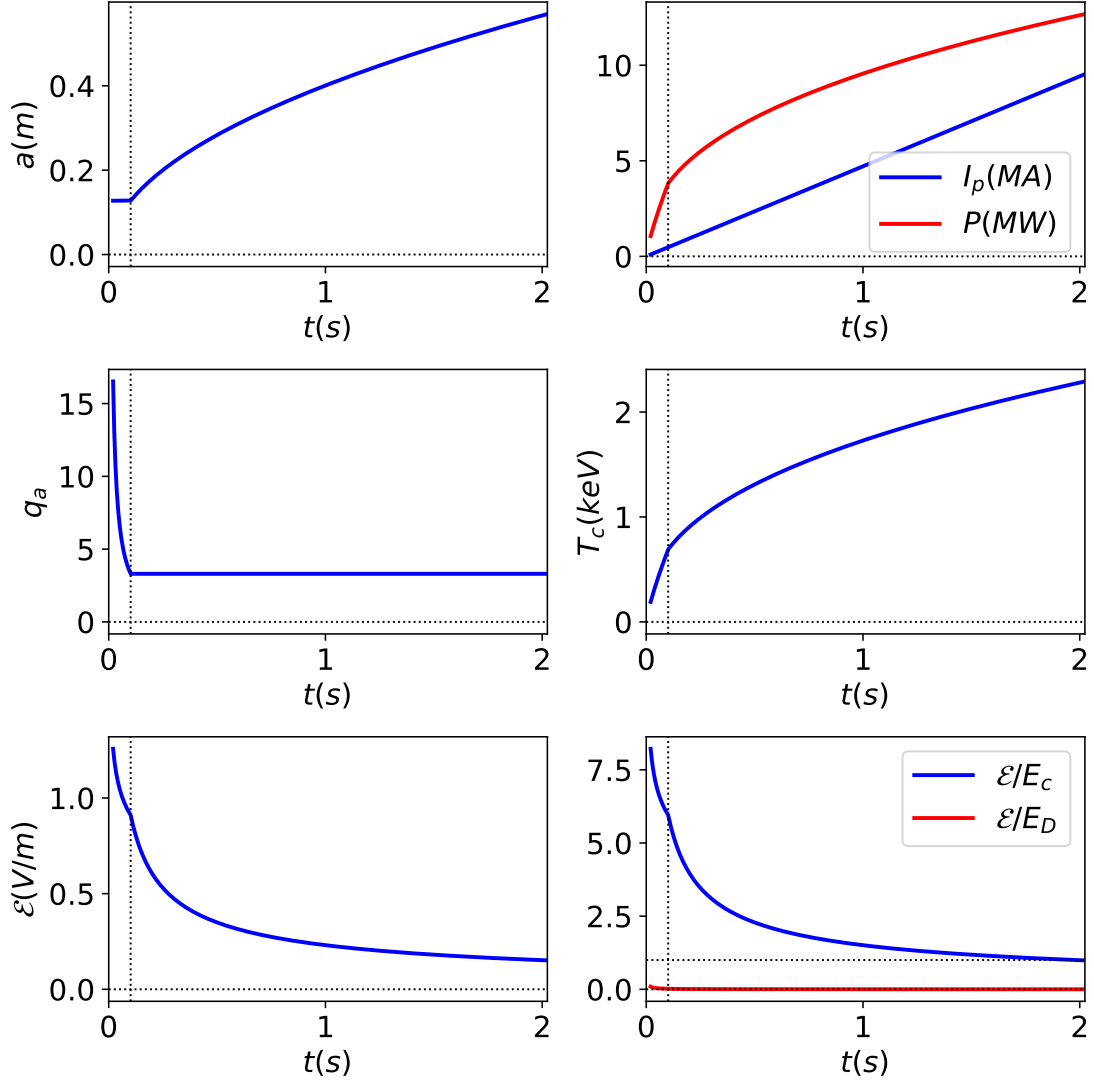
FIG. 5. Simulated current ramp-up for the SPARC tokamak. See caption to Fig. 4.
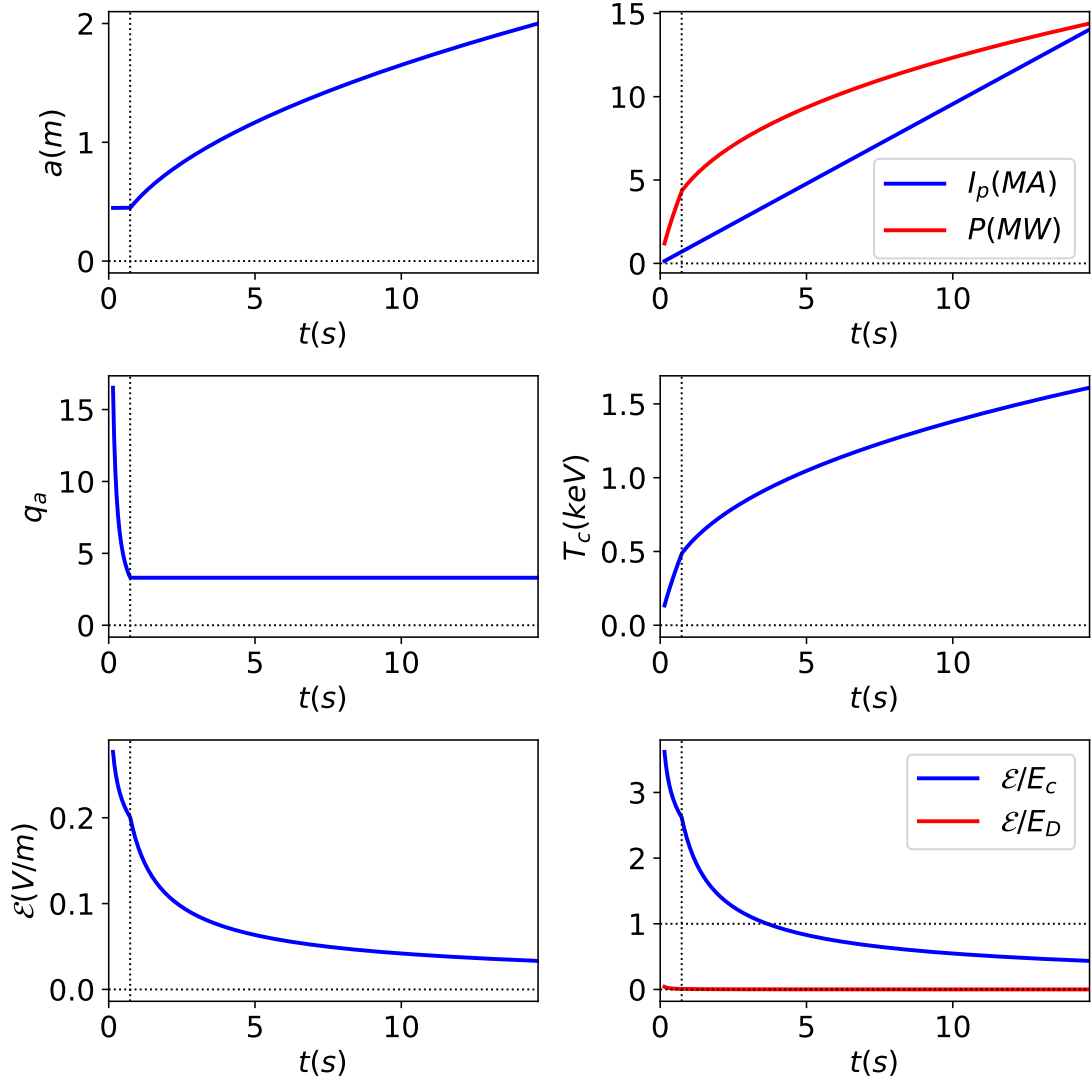
FIG. 6. Simulated current ramp-up for the ITER tokamak. See caption to Fig. 4.